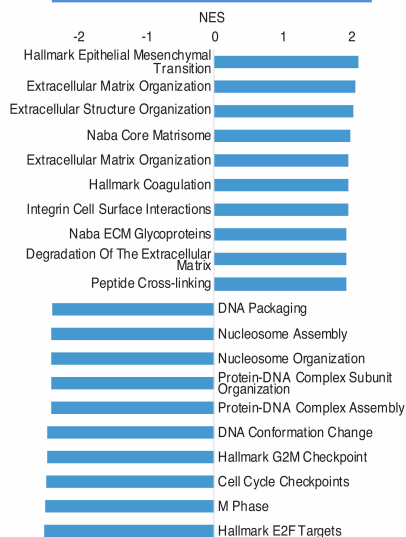
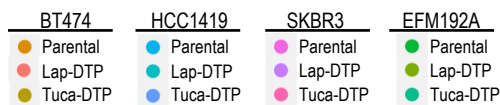
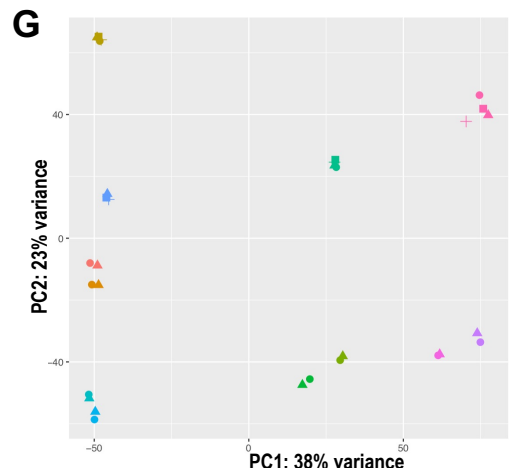
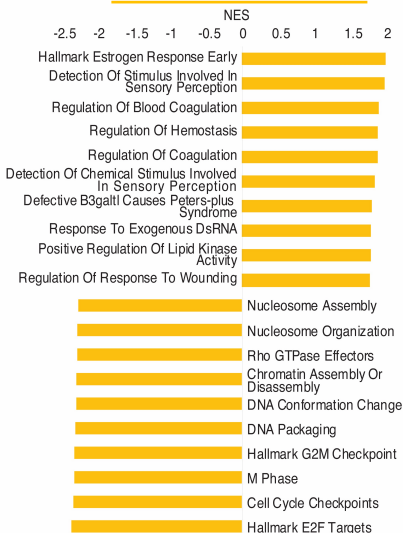


Supplementary Fig. S1

A Mesenchymal-like DTP GSEA



B Luminal-like DTP GSEA



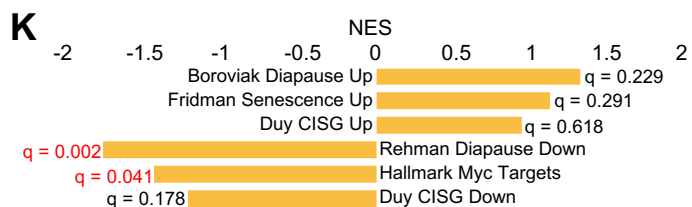
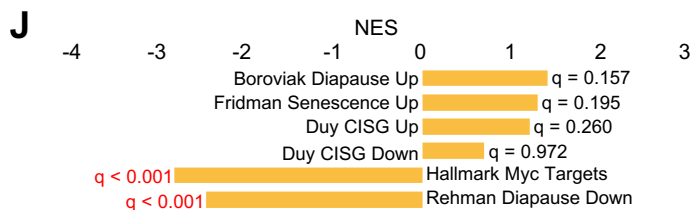
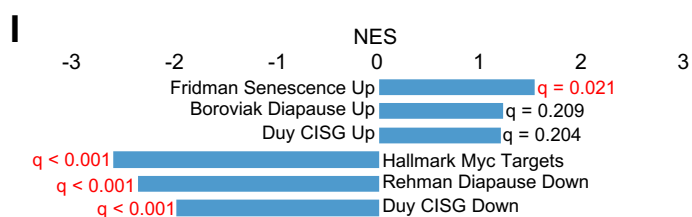
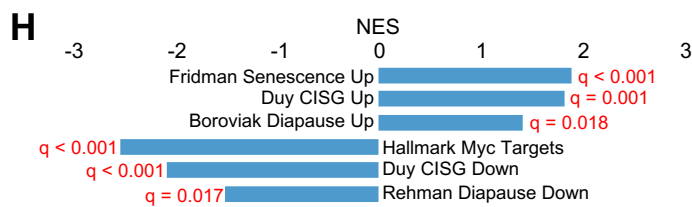
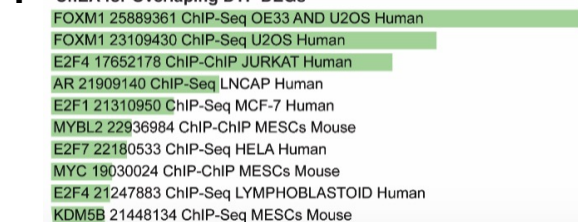
D ChEA for Mesenchymal DTP Unique DEGs



E ChEA for Luminal DTP Unique DEGs

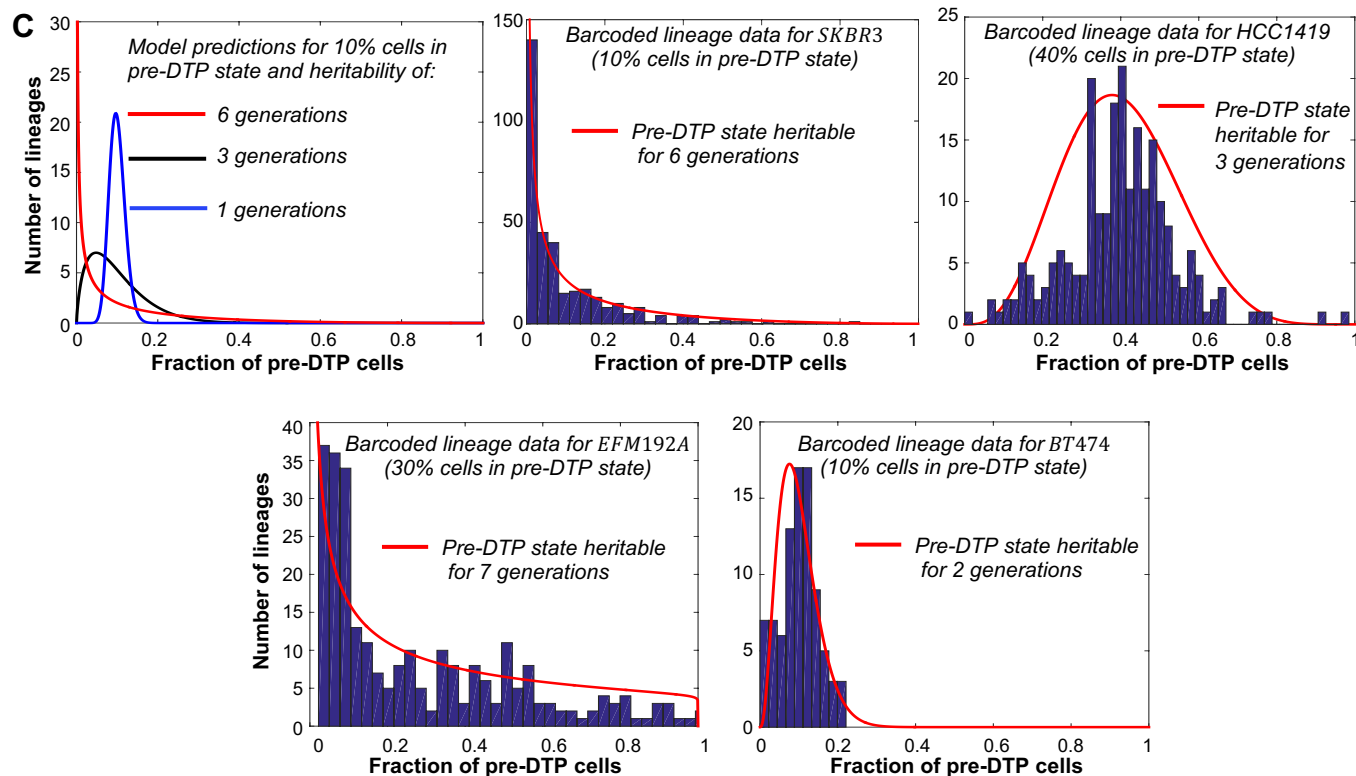
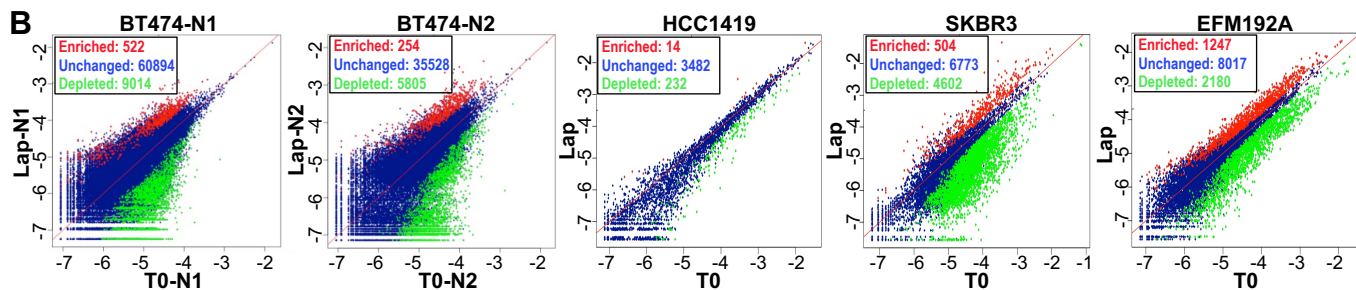
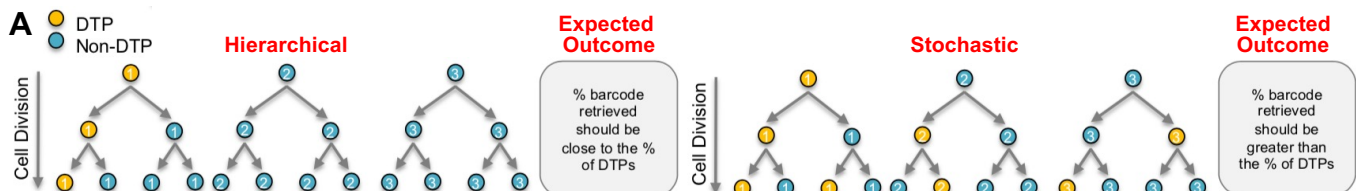


F ChEA for Overlapping DTP DEGs



Supplementary Fig. S1. HER2 TKI DTPs exhibit two distinct transcriptional programs, related to Figure 2. A and B, Top and bottom ten enriched GSEA terms for differentially expressed genes (DEGs) between lapatinib-DTPs and parental cells in the mesenchymal-like (**A**) and luminal-like (**B**) subgroups. **C,** Venn diagram showing overlap of DEGs (compared with cognate parental cells) from mesenchymal-like and luminal-like DTPs. The non-overlapping genes are termed “mesenchymal DTP unique DEGs” (796 genes) and “luminal DTP unique DEGs” (313 genes). **D-F,** TF binding site enrichment, as predicted by ChEA, is displayed for the mesenchymal DTP unique DEGs (**D**), luminal DTP unique DEGs (**E**), and overlapping DEGs (**F**), respectively. Bars indicate ChEA combined score. **G,** Principal component analysis (PCA) of parental cells, lapatinib-DTPs and tucatinib-DTPs from BT474, HCC1419, SKBR3, and EFM192A lines. **H-K,** GSEA for the indicated signatures examined in mesenchymal-like lapatinib-DTPs (**H**), mesenchymal-like tucatinib-DTPs (**I**), luminal-like lapatinib-DTPs (**J**), and luminal-like tucatinib-DTPs (**K**).

Supplementary Fig. S2



Supplementary Fig. S2. Barcoding experiments indicate stochastic origin of lapatinib-DTPs, related to Figure 3. **A**, Schematic shows potential models of DTP ontogeny and expected outcomes of barcoding experiments. **B**, Plots show distributions of barcodes expressed as Log(clone frequency) from T0 and 14d lapatinib-treated cells. Red indicates significantly enriched barcodes, green indicates significantly depleted barcodes, and blue shows unchanged barcodes after 14d lapatinib treatment (DTPs). **C**, Model-predicted lineage-to-lineage fluctuations in the fraction of pre-DTPs for different transient heritability of the pre-DTP state. Longer heritability drives enhanced fluctuations (Top left). Distribution of pre-DTPs as obtained from barcoding lineage data from the four cell lines. The corresponding model fits (solid red lines) reveal the pre-DTP state heritability for each cell line.

Supplementary Fig. S3

A Cluster A: GO Biological Process Enrichment

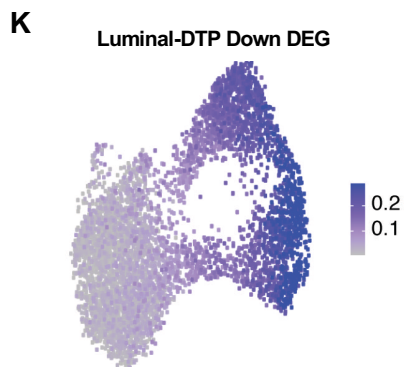
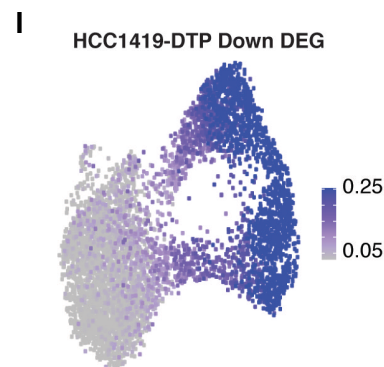
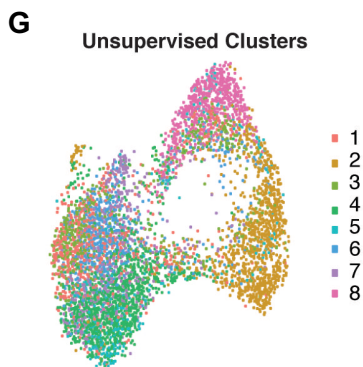
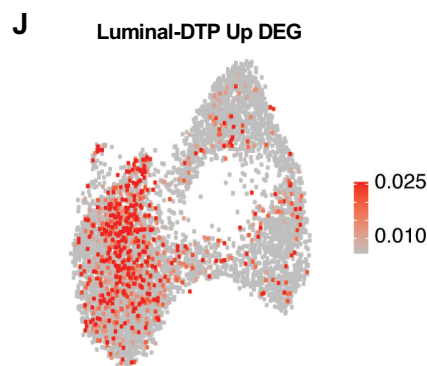
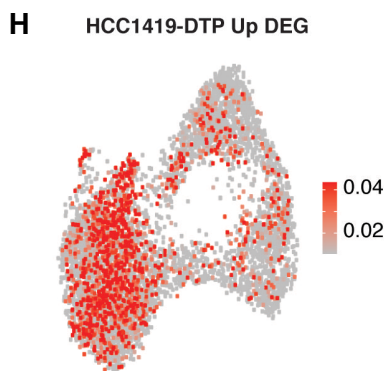
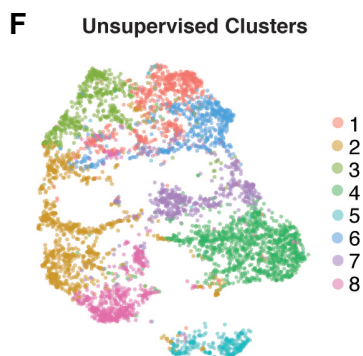
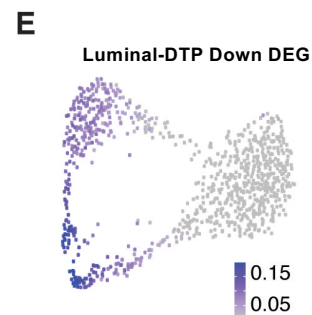
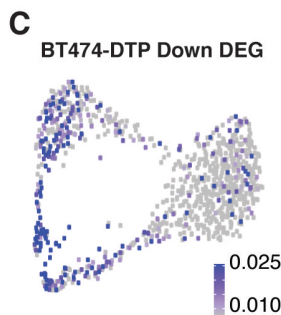
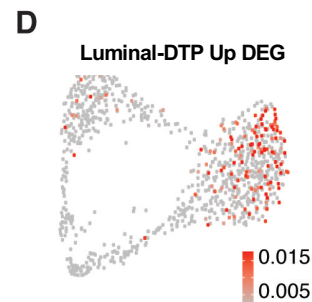
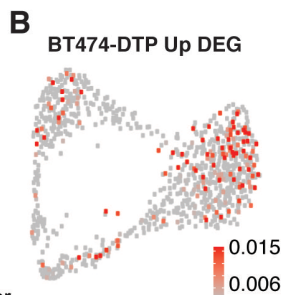
DNA metabolic process
 DNA replication
 DNA repair
 G1/S transition of mitotic cell cycle
 cellular response to DNA damage stimulus
 mitotic cell cycle phase transition
 DNA-dependent DNA replication
 cell cycle G1/S phase transition
 DNA synthesis involved in DNA repair
 cellular macromolecule biosynthetic process

Cluster B: GO Biological Process Enrichment

negative regulation of transcription from RNA polymerase II promoter
 regulation of cell size
 negative regulation of cell proliferation
 negative regulation of wound healing
 phosphatidylinositol phosphorylation
 negative regulation of cell motility
 negative regulation of transcription, DNA-templated
 regulation of phosphatidylinositol 3-kinase activity
 lipid phosphorylation
 regulation of filopodium assembly

Cluster C: GO Biological Process Enrichment

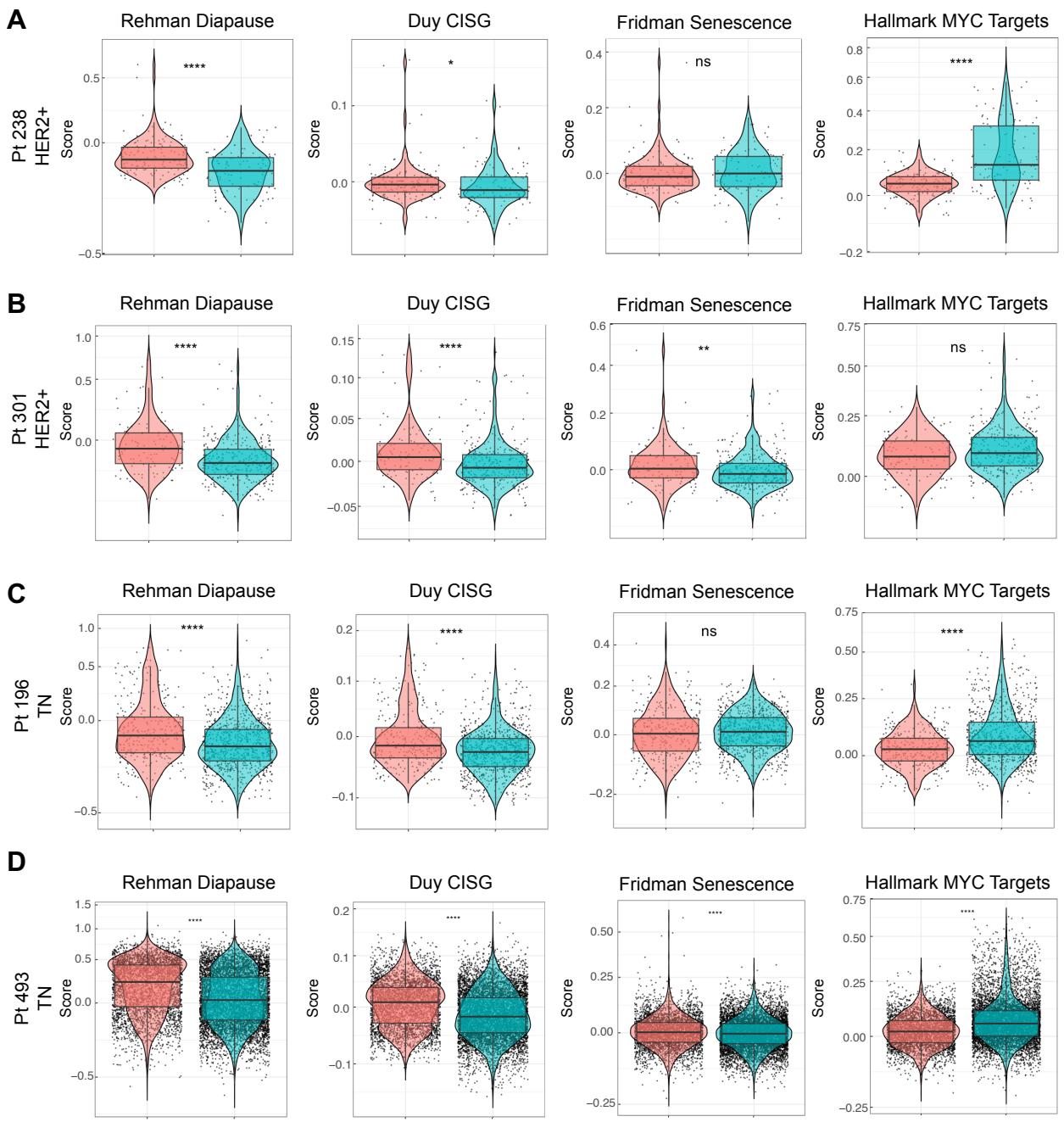
regulation of mitotic cell cycle phase transition
 mitotic sister chromatid segregation
 regulation of G2/M transition of mitotic cell cycle
 anaphase-promoting complex-dependent catabolic process
 positive regulation of ubiquitin protein ligase activity
 RNA splicing, via transesterification reactions with bulged adenosine as nucleophile
 mRNA splicing, via spliceosome
 regulation of ubiquitin-protein ligase in regulation of mitotic cell cycle transition
 regulation of ubiquitin-protein ligase activity involved in mitotic cell cycle
 mitotic cell cycle phase transition



Supplementary Fig. S3. Single-cell RNA-sequencing reveals sub-population enriched for lapatinib DTP genes in untreated HER2+ breast cancer cells, related to Figure 3. **A**, GO Biological Process enrichment for unsupervised clusters of untreated BT474 cells. **B-E**, UMAP of supervised clustering of untreated BT474 cells using cell cycle signature genes defined by Xue *et al.* (44). Cells are colored by BT474-DTP Up (**B**) or Down (**C**) DEG expression or by luminal-DTP Up (**D**) or Down (**E**) DEG expression. Scale shows the signature expression score for each. **F**, UMAP showing the results of unsupervised clustering of untreated HCC1419 cells. Each unsupervised cluster is represented by a number and color, as indicated. **G**, UMAP showing supervised clustering of untreated HCC1419 cells with cell cycle signature genes defined by Xue *et al.* (44), colored by the unsupervised clusters in **F**. **H-K**, UMAP showing supervised clustering of untreated HCC1419 with Xue *et al.* cell cycle genes (44), with cells colored by HCC1419-DTP Up (**H**) or Down (**I**) DEG expression or luminal-like DTP Up (**J**) or Down (**K**) DEG expression. Scale shows the signature expression score for each.

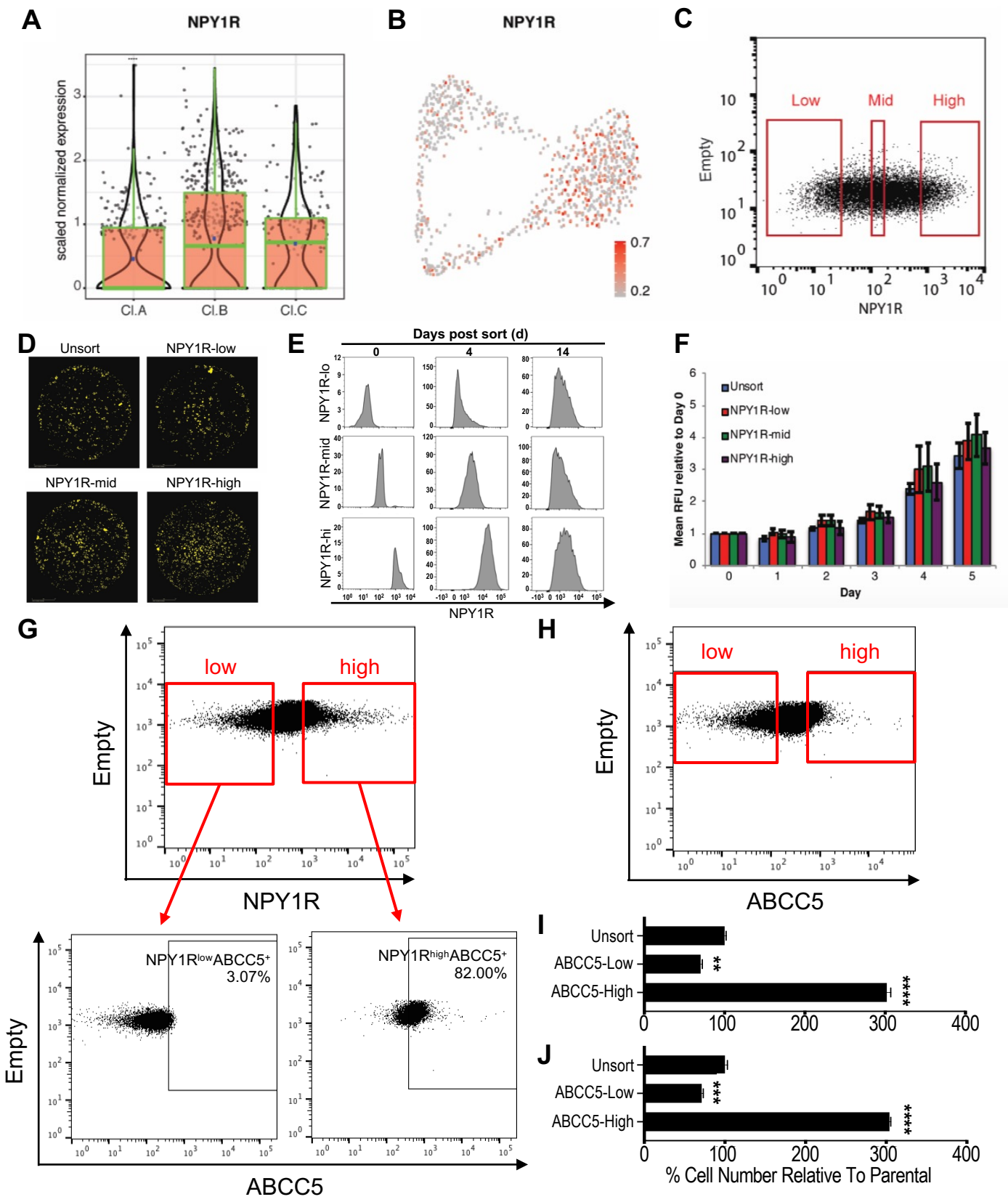
Supplementary Fig. S4

G0
Non G0



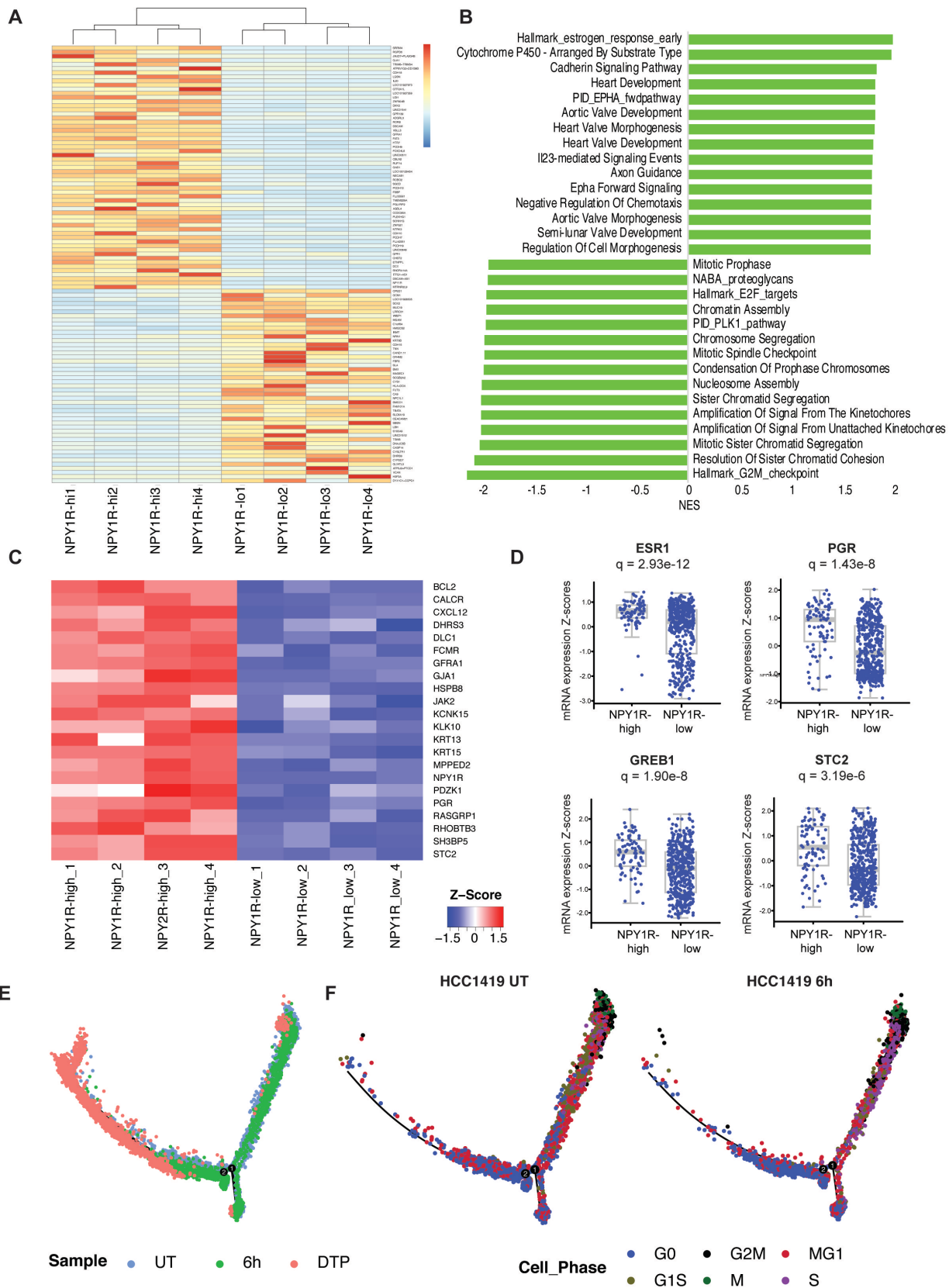
Supplementary Fig. S4. G₀ cells from treatment-naive primary breast tumors are enriched for diapause genes, chemotherapy-induced stress, and senescence genes, related to Figure 4. Signature scores for Rehman_Diapause_UP, Duy_CISG_UP, Fridman_Senescence_UP, and Hallmark_of MYC_targets in HER2+ tumors from Pt238 (A) and Pt301 (B), and from TNBC tumors from Pt196 (C) and Pt493 (D).

Supplementary Fig. S5



Supplementary Fig. S5. Enrichment of pre-DTPs from untreated BT474 cells by FACS for NPY1R and ABCC5, related to Figure 5. **A**, *NPY1R* expression in unsupervised clusters from untreated BT474 cells. **B**, UMAP showing supervised clustering of untreated BT474 single cells by their cell cycle gene expression with cells colored by *NPY1R* expression level. **C**, Plot showing *NPY1R* levels in untreated BT474 cells and gates used to define *NPY1R*^{hi}, *NPY1R*^{mid}, and *NPY1R*^{lo} fractions. **D**, FACS-isolated cells from the indicated *NPY1R* fractions were treated with lapatinib for 14 days and then cultured in drug-free media for 14 days. Representative Incucyte images at the experimental endpoint are displayed, and a color mask is applied to show residual cells. **E**, *NPY1R*^{hi}, *NPY1R*^{mid}, and *NPY1R*^{lo} BT474 cells were isolated by FACS and cultured under standard conditions. *NPY1R* expression was assessed by flow cytometry post-sort (Day 0) and at Days 4 and 14 of culture. **F**, FACS-isolated *NPY1R* cells were cultured under standard conditions, and viable cell number was quantified by Alamar Blue assay at the indicated times. Alamar Blue readings (RFU) were compared to the Day 0 values for each sample. **G**, Plot showing *NPY1R* levels in untreated BT474 cells and gates used to define *NPY1R*^{hi} and *NPY1R*^{lo} fractions (upper panel). *ABCC5* expression is shown for *NPY1R*^{hi} (lower right) and *NPY1R*^{lo} (lower left) cells. **H-J**, *ABCC5*^{hi} and *ABCC5*^{lo} BT474 cells were isolated by FACS (**H**) and treated with lapatinib (**I**) or tucatinib (**J**) for 14 days. Cells were counted and compared to unsorted control cells. Mean \pm SEM from three independent experiments is shown. Significance was assessed by one-way ANOVA with Tukey multiple comparisons test (** $p < 0.01$, *** $p < 0.001$, **** $p < 0.0001$).

Supplementary Fig. S6

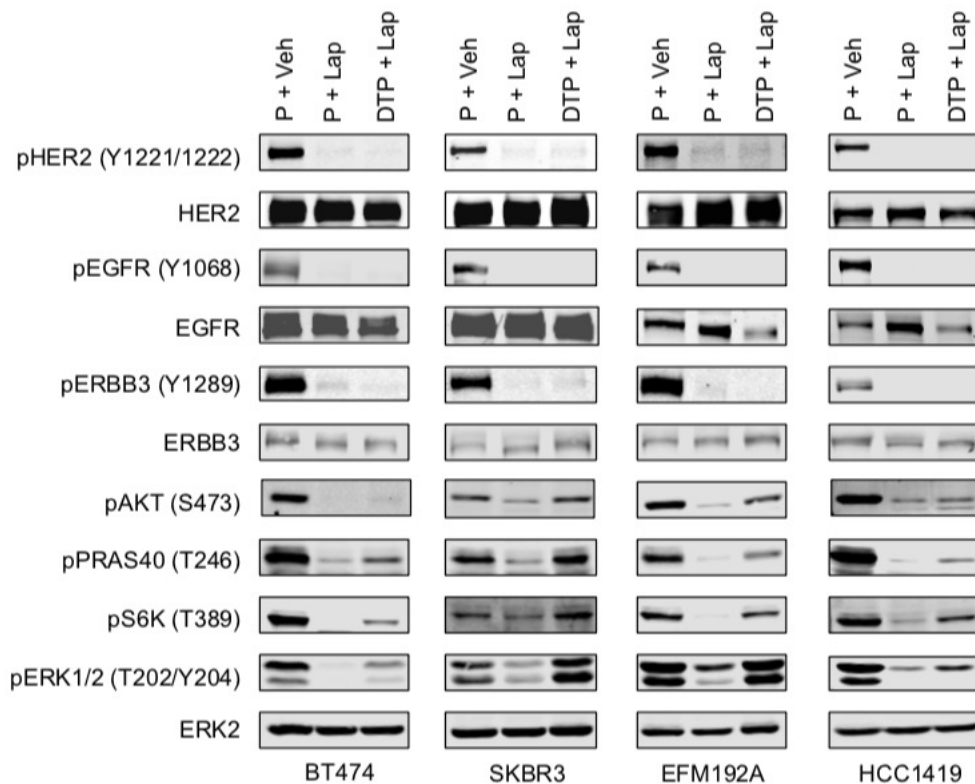


Supplementary Fig. S6. NPY1R^{hi} cells have enhanced basal estrogen receptor (ER) activity and HCC1419 G₀ cells are on trajectory to become DTPs, related to Figure 5.

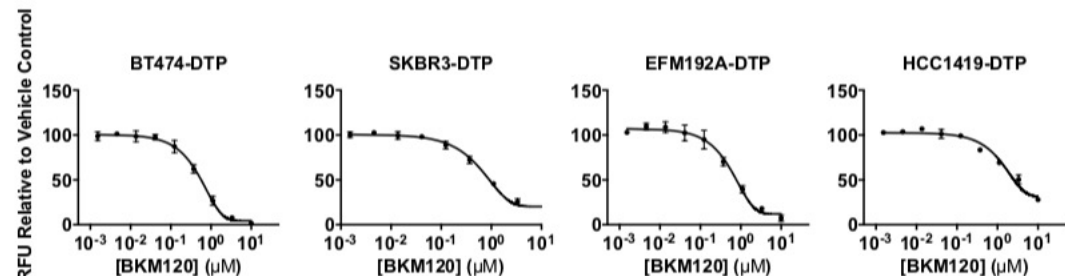
A, Heatmap showing DEGs from NPY1R^{hi}, compared with NPY1R^{lo}, cells. Scale represents z-score. **B,** Top ten positively and negatively enriched GSEA terms, ranked by normalized enrichment score (NES), for DEGs in FACS-isolated NPY1R^{hi} vs. NPY1R^{lo} BT474 cells. **C,** Heatmap showing ER targets enriched in NPY1R^{hi} compared with NPY1R^{lo} cells. Scale represents z-score. **D,** Expression of ER targets in NPY1R^{hi} vs. NPY1R^{lo} breast tumors from TCGA. NPY1R^{hi} tumors are defined as those with *NPY1R* expression 1 SD above the mean; all other tumors are considered NPY1R^{lo}. The q value was calculated by the Benjamini-Hochberg procedure. **E,** Pseudotime analysis of untreated and 6h lapatinib-treated HCC1419 cells and HCC1419 DTPs with cells colored by sample. **F,** Respective positions of untreated and 6h lapatinib-treated HCC1419 cells on the pseudotime trajectory, with cells colored by cell cycle phase, as defined by the Xue *et al.* (44).

Supplementary Fig. S7

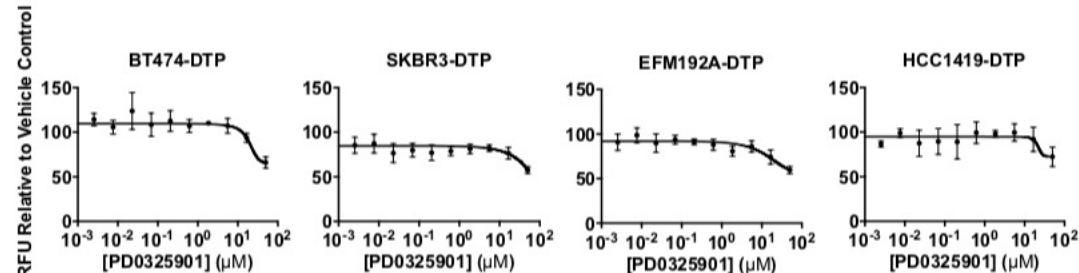
A



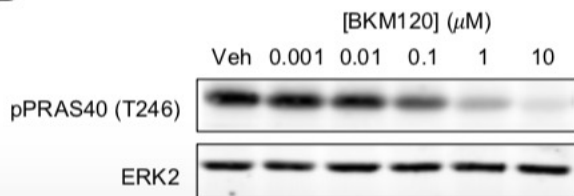
B



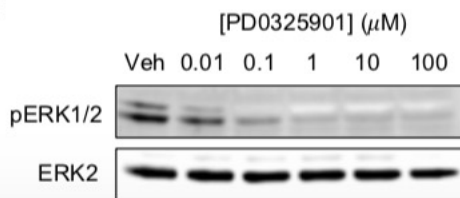
C



D

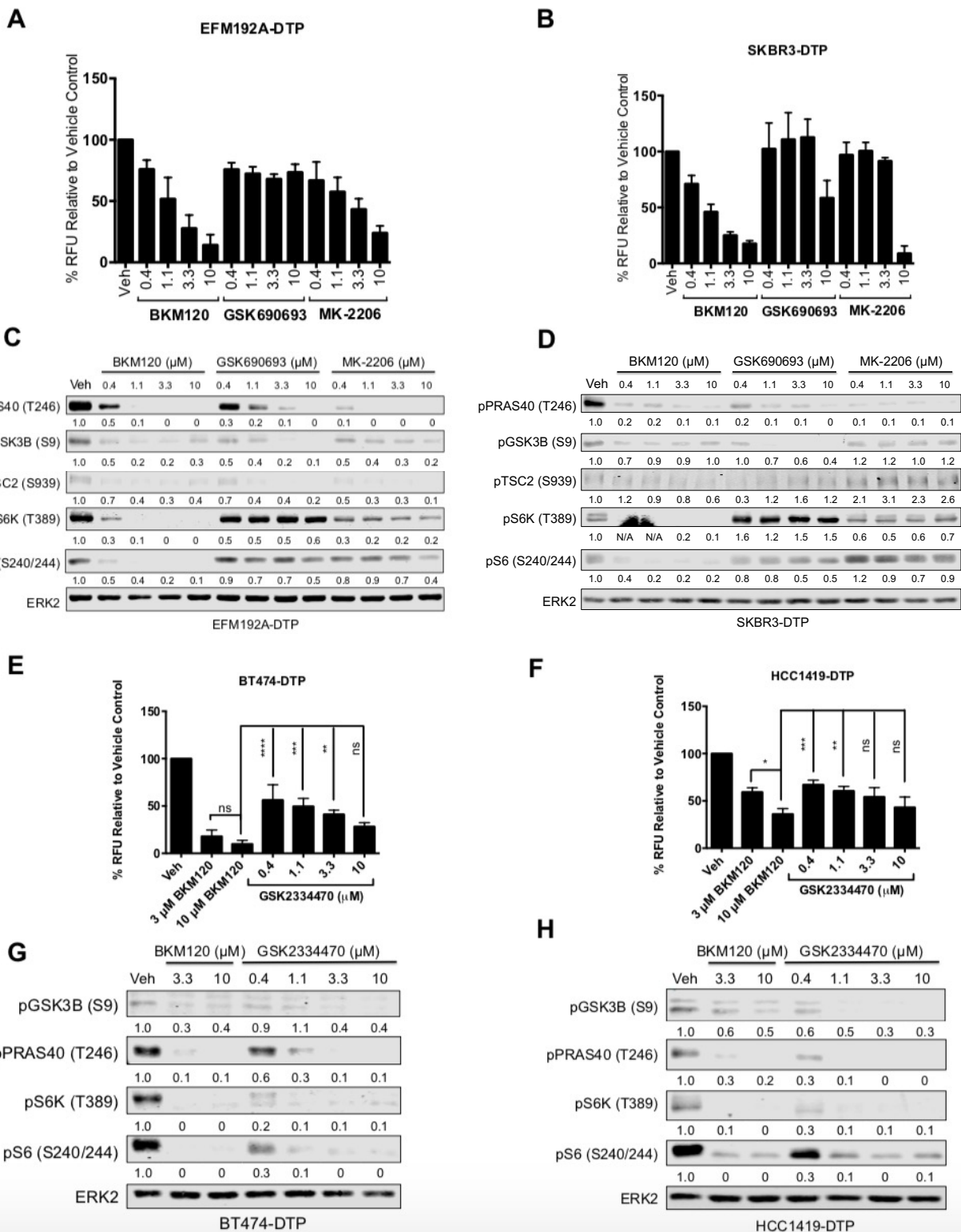


E



Supplementary Fig. S7. PI3K and ERK/MAPK pathways are re-activated in lapatinib-DTPs, but only PI3K pathway is required for lapatinib-DTP survival, related to Figure 6. A, Parental cells (P) were treated with vehicle or 2.5 μ M lapatinib for one hour (P + lap) and compared with lapatinib-DTPs cultured continuously in 2.5 μ M lapatinib. Downstream signaling events were assessed by immunoblotting with the indicated phospho-specific antibodies. ERK2 serves as a loading control. **B** and **C,** Lapatinib-DTPs were treated with the pan-PI3K inhibitor BKM120 (**B**) or the MEK inhibitor PD0325901 (**C**) for 96 hours. Surviving cells were quantified by Alamar Blue viability assay. Mean \pm SEM of normalized relative fluorescence units (RFU) from three independent experiments is displayed. **D** and **E,** EFM192A lapatinib-DTPs were treated with the indicated doses of BKM120 (**D**) and PD0325901 (**E**) for one hour, and whole cell lysates were analyzed by immunoblotting to assess pathway inhibition. ERK2 serves as a loading control.

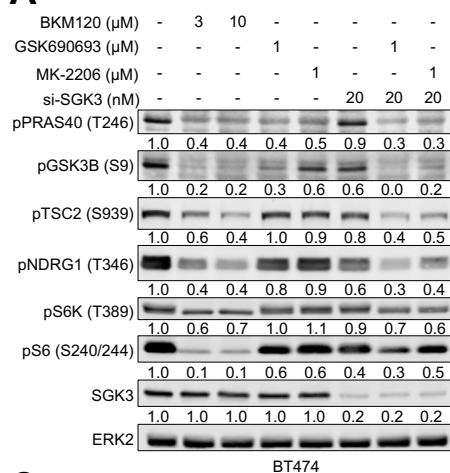
Supplementary Fig. S8



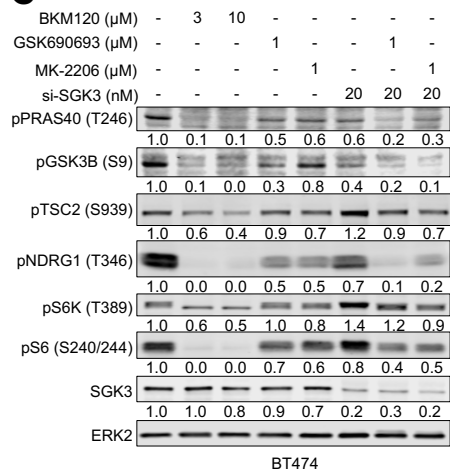
Supplementary Fig. S8. Mesenchymal-like lapatinib-DTPs also are more sensitive to PI3K than to AKT inhibition and mTORC1 activation and survival in luminal-like lapatinib-DTP are dependent on PDK1, related to Figure 6. **A** and **B**, Lapatinib-DTPs from EFM192A (**A**) and SKBR3 (**B**) cells were treated with increasing doses of BKM120, GSK690693, or MK-2206 for 96 hours, and surviving cells were quantified by Alamar Blue viability assay. Mean \pm SEM of normalized relative fluorescence units (RFU) from three independent experiments is shown. **C** and **D**, EFM192A (**C**) and SKBR3 (**D**) DTPs were treated as indicated for one hour, and whole cell lysates were analyzed by immunoblotting with the indicated antibodies. Numbers under the blots indicate relative intensities compared to the vehicle control. **E** and **F**, Lapatinib-DTPs from BT474 (**E**) and HCC1419 (**F**) cells were treated with indicated doses of BKM120 or the PDK1 inhibitor GSK2334470 for 96 hours, and surviving cells were quantified by Alamar Blue. Mean \pm SEM of normalized relative fluorescence units (RFU) from three independent experiments is displayed. (ns, $p>0.05$, $*p<0.05$; $**p<0.01$, $***p<0.001$, $****p<0.0001$, one-way ANOVA, with Tukey multiple comparisons test). **G** and **H**, Lapatinib-DTPs from BT474 (**G**) and HCC1419 (**H**) cells were treated as indicated for one hour, and whole cell lysates were subjected to immunoblotting. Numbers under the blots indicate relative intensities compared to vehicle control.

Supplementary Fig. S9

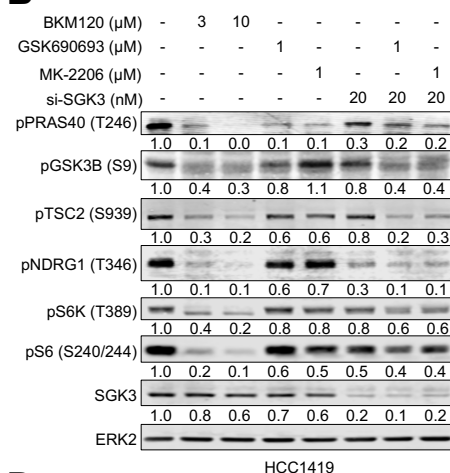
A



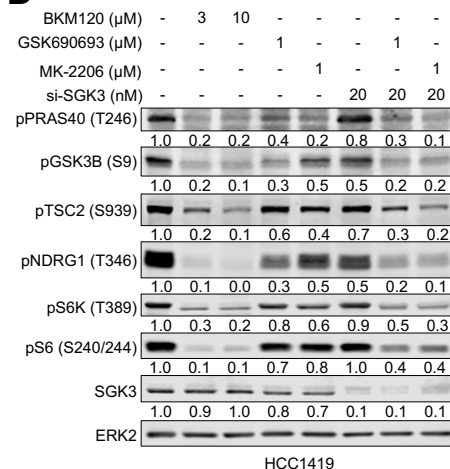
C



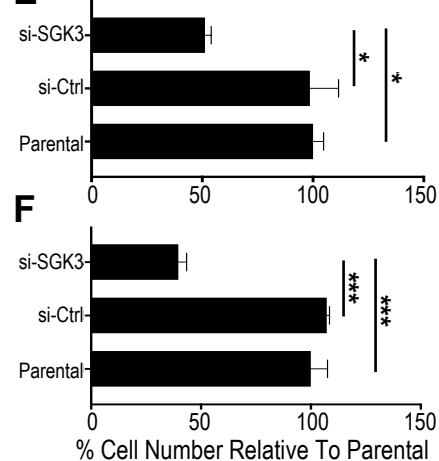
B



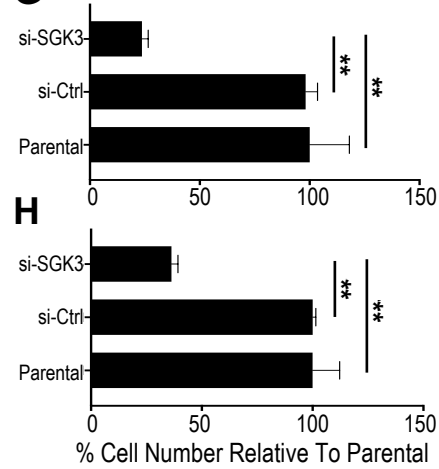
D



E



F



G



H



Supplementary Fig. S9. SGK3 knockdown plus AKT inhibition ablates AKT-independent TSC2 phosphorylation and mTORC1 activation and reduces survival of cells in response to HER2 TKIs. A and B, SGK3 was depleted by using siRNA (si-SGK3) in BT474 (A) and HCC1419 (B) for 72 hours before treatment with lapatinib for another 72 hours. Cells were then treated with 3 μ M or 10 μ M BKM120, 1 μ M GSK690693, or 1 μ M MK-2206 as indicated for one hour, and whole cell lysates were subjected to immunoblot analysis with the indicated antibodies. Numbers under the blots indicate relative intensity compared to the vehicle control. Representative blots from one of two independent experiments are displayed. C and D, Same as A and B except cells were treated with tucatinib. Representative blots from one of two independent experiments are displayed. E-H, Parental BT474 (E, G) and HCC1419 (F, H) cells or BT474 and HCC1419 cells transfected with si-Ctrl or si-SGK3 for 72 hours were treated with lapatinib (E and F) or tucatinib (G and H) for 14 days. Cells were counted and compared to parental control. Mean \pm SEM from three independent experiments is shown. Significance was assessed by one-way ANOVA with Tukey multiple comparisons test (* p <0.05, ** p < 0.01, * p <0.001).**